

# Hepatic Deletion of Janus Kinase 2 Counteracts Oxidative Stress in Mice

Madeleine Themanns, Kristina Mueller, Sonja Kessler, Nicole Golob-Schwarzl, Thomas Mohr, Doris Kaltenecker, Jerome Bourgeais, Jamile Paier-Pourani, Katrin Friedbichler, Doris Schneller, et al.

▶ **To cite this version:**

Madeleine Themanns, Kristina Mueller, Sonja Kessler, Nicole Golob-Schwarzl, Thomas Mohr, et al.. Hepatic Deletion of Janus Kinase 2 Counteracts Oxidative Stress in Mice. Scientific Reports, 2016, 6 (1), 10.1038/srep34719 . hal-02411728

**HAL Id: hal-02411728**

**https://univ-tours.hal.science/hal-02411728**

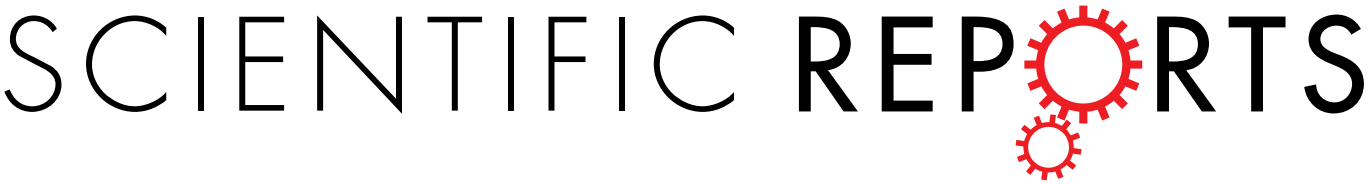
Submitted on 30 Oct 2021

**HAL** is a multi-disciplinary open access archive for the deposit and dissemination of scientific research documents, whether they are published or not. The documents may come from teaching and research institutions in France or abroad, or from public or private research centers.

L'archive ouverte pluridisciplinaire **HAL**, est destinée au dépôt et à la diffusion de documents scientifiques de niveau recherche, publiés ou non, émanant des établissements d'enseignement et de recherche français ou étrangers, des laboratoires publics ou privés.



Distributed under a Creative Commons Attribution 4.0 International License



OPEN

# Hepatic Deletion of Janus Kinase 2 Counteracts Oxidative Stress in Mice

Received: 02 June 2016
Accepted: 19 September 2016
Published: 07 October 2016

Madeleine Themanns[1,2], Kristina M. Mueller[1,2], Sonja M. Kessler[3], Nicole Golob-Schwarzl[4], Thomas Mohr[5], Doris Kaltenecker[1,2], Jerome Bourgeais[6], Jamile Paier-Pourani[7], Katrin Friedbichler[1], Doris Schneller[5], Michaela Schlederer[1,8], Eva Zebedin-Brandl[9], Luigi M. Terracciano[10], Xiaonan Han[11], Lukas Kenner[1,8,12], Kay-Uwe Wagner[13], Wolfgang Mikulits[5], Andrey V. Kozlov[7], Markus H. Heim[14], Fabrice Gouilleux[6], Johannes Haybaeck[15] & Richard Moriggl[1,2,16]

**Genetic deletion of the tyrosine kinase JAK2 or the downstream transcription factor STAT5 in liver impairs growth hormone (GH) signalling and thereby promotes fatty liver disease. Hepatic STAT5 deficiency accelerates liver tumourigenesis in presence of high GH levels. To determine whether the upstream kinase JAK2 exerts similar functions, we crossed mice harbouring a hepatocyte-specific deletion of JAK2 (JAK2$^{\Delta hep}$) to GH transgenic mice (GH$^{tg}$) and compared them to GH$^{tg}$STAT5$^{\Delta hep}$ mice. Similar to GH$^{tg}$STAT5$^{\Delta hep}$ mice, JAK2 deficiency resulted in severe steatosis in the GH$^{tg}$ background. However, in contrast to STAT5 deficiency, loss of JAK2 significantly delayed liver tumourigenesis. This was attributed to: (i) activation of STAT3 in STAT5-deficient mice, which was prevented by JAK2 deficiency and (ii) increased detoxification capacity of JAK2-deficient livers, which diminished oxidative damage as compared to GH$^{tg}$STAT5$^{\Delta hep}$ mice, despite equally severe steatosis and reactive oxygen species (ROS) production. The reduced oxidative damage in JAK2-deficient livers was linked to increased expression and activity of glutathione S-transferases (GSTs). Consistent with genetic deletion of *Jak2*, pharmacological inhibition and siRNA-mediated knockdown of *Jak2* led to significant upregulation of *Gst* isoforms and to reduced hepatic oxidative DNA damage. Therefore, blocking JAK2 function increases detoxifying GSTs in hepatocytes and protects against oxidative liver damage.**

Non-alcoholic fatty liver disease (NAFLD) is becoming the most common chronic liver disease and represents an enormous public health problem. Accumulation of ectopic lipids in liver is the hallmark of NAFLD. Its histologic spectrum ranges from simple steatosis to the progressive form of non-alcoholic steatohepatitis (NASH), which might further progress to cirrhosis and its related complications, such as hepatocellular carcinoma (HCC)[1–3]. There is evidence that HCC can develop in NAFLD patients even without cirrhosis, suggesting an association between abnormal metabolic processes and HCC[2,4–6]. Increased generation of reactive oxygen species (ROS) is found in patients and mouse models with NAFLD[6–11]. When the equilibrium between ROS generation and the

[1]Ludwig Boltzmann Institute for Cancer Research, Vienna, Austria. [2]Institute of Animal Breeding and Genetics, University of Veterinary Medicine, Vienna, Austria. [3]Department of Pharmacy, Pharmaceutical Biology, Saarland University, Saarbrücken, Germany. [4]Center for Biomarker Research in Medicine, Graz, Austria. [5]Institute of Cancer Research, Department of Medicine I, Comprehensive Cancer Center, Medical University of Vienna, Vienna, Austria. [6]François Rabelais University, CNRS UMR 7292, LNOx team, Tours, France. [7]Ludwig Boltzmann Institute for Experimental and Clinical Traumatology in AUVA Center, Vienna, Austria. [8]Institute of Clinical Pathology, Medical University of Vienna, Vienna, Austria. [9]Institute of Pharmacology, Centre of Physiology and Pharmacology, Medical University of Vienna, Vienna, Austria. [10]Molecular Pathology Division, Institute of Pathology, University Hospital of Basel, Basel, Switzerland. [11]Division of Gastroenterology, Hepatology and Nutrition, Cincinnati Children's Hospital Medical Center, Cincinnati, OH, USA. [12]Unit of Pathology of Laboratory Animals, University of Veterinary Medicine, Vienna, Austria. [13]Eppley Institute for Research in Cancer and Allied Diseases, University of Nebraska Medical Center, Omaha, USA. [14]Department of Biomedicine, University Hospital Basel, Basel, Switzerland. [15]Institute of Pathology, Medical University of Graz, Graz, Austria. [16]Medical University of Vienna, Vienna, Austria. Correspondence and requests for materials should be addressed to R.M. (email: richard.moriggl@lbicr.lbg.ac.at)

antioxidant defence is disrupted, the resulting oxidative stress promotes liver injury, which increases the risk for HCC development[7].

Growth hormone (GH) affects whole-body physiology via the widely expressed GH receptor (GHR). In the liver GH activates the Janus kinase (JAK) 2 and signal transducer and activator of transcription (STAT) 5 signalling pathway to regulate target genes involved in vital liver functions[12]. GH-deficient or GH-resistant states both cause impaired signal transduction through the GHR in liver and this correlates with chronic liver disease including NAFLD[13–16]. Similarly, mice lacking components of the GHR-JAK2-STAT5 axis in hepatocytes develop hepatic GH resistance and steatosis[17–21]. We and others identified hepatic STAT5 deficiency as being associated with higher susceptibility to liver cancer[20,22–24], driven through progressive steatosis.

Here, we addressed the impact of hepatic JAK2 deficiency on the progression of hepatic steatosis. Furthermore, we aimed to elucidate the contribution of hepatic JAK2 and STAT5 deficiency to oxidative stress with consequence for HCC development in a situation of hyperactived GH signalling. Therefore, we crossed mice harbouring a hepatocyte-specific deletion of either JAK2 or STAT5 ($JAK2^{\Delta hep}$, $STAT5^{\Delta hep}$; using AlfpCre[24,25]) to growth hormone transgenic mice ($GH^{tg}$)[26]. $GH^{tg}$ mice display high systemic circulating levels of GH that are causally related to a sustained increase in hepatocyte turnover and hyperplasia followed by development of hepatocellular tumours[26].

Consistent with previous findings[18,21], JAK2 deficiency caused hepatic steatosis by inducing lipid redistribution to the liver and hepatic lipid synthesis. Yet, despite profound steatosis in $GH^{tg}JAK2^{\Delta hep}$ mice, liver tumourigenesis was delayed as compared to $GH^{tg}STAT5^{\Delta hep}$. While accelerated tumourigenesis in STAT5-deficient mice was associated with aberrant activation of STAT3 and increased oxidative damage, delayed carcinogenesis in JAK2-deficient mice was linked to reduced STAT3 signalling and ROS-induced oxidative damage.

## Results

**JAK2 deficiency promotes hepatic steatosis by ectopic lipid redistribution and *de novo* lipogenesis.** JAK2 deficiency alone and in combination with hyperactivated GH signalling resulted in severe hepatic steatosis and a reduction in body weight, which is consistent with previous reports[18,21]. The reduction in body weight remained at approximately 20% in both JAK2-deficient lines compared to WT mice at 12 and 40 weeks of age, while body weights of $GH^{tg}$ mice were increased (Fig. 1a). Hepatomegaly was already evident in 12-week old $GH^{tg}JAK2^{\Delta hep}$ animals. At 40 weeks of age, $GH^{tg}JAK2^{\Delta hep}$ mice displayed increased liver weight (LW) to body weight (BW) ratios of 15% compared to WT mice, while LW/BW ratios of $GH^{tg}$ and $JAK2^{\Delta hep}$ mice were elevated by 10% (Fig. 1b). Furthermore, in comparison to WT mice, serum levels of alanine aminotransferase (ALT) and aspartate-aminotransferase (AST) were elevated in all genotypes as indicators of liver damage (Fig. 1c). Subsequent histopathological analysis confirmed severe steatosis in both $GH^{tg}JAK2^{\Delta hep}$ and $JAK2^{\Delta hep}$ mice characterised by medio- to macro- and microvesicular steatosis (Fig. 1d), which was accompanied by mild lobular inflammation at 40 weeks of age when compared to WT littermates (Supplementary Fig. S1a). Particularly, microvesicular steatosis was more prominent in livers of young and aged $GH^{tg}JAK2^{\Delta hep}$ mice (Fig. 1e, Supplementary Fig. S1a). Electron microscopy analysis revealed big and swollen mitochondria in $GH^{tg}JAK2^{\Delta hep}$ and $JAK2^{\Delta hep}$ livers (Supplementary Fig. S1b), indicating mitochondrial dysfunction and fatty degeneration in hepatocytes.

Next, we investigated the consequences of JAK2 deficiency for lipid metabolism. In $GH^{tg}JAK2^{\Delta hep}$ animals, high GH levels led to massive lysis of perigonadal white adipose tissue (WAT), which was not affected in $JAK2^{\Delta hep}$ mice (Fig. 2a). Lipolysis was manifested by a reduction of WAT/BW ratios over time and an increase in circulating free fatty acids (FFAs). This coincided with greatly elevated protein levels of FA translocase CD36 in $JAK2^{\Delta hep}$ and $GH^{tg}JAK2^{\Delta hep}$ livers, indicating an increased capability of hepatic FFA uptake[18,27]. Furthermore, significantly elevated serum triglyceride (TG) levels, were found in $JAK2^{\Delta hep}$ and $GH^{tg}JAK2^{\Delta hep}$ mice (Fig. 2a), indicative of hypertriglyceridemia[28]. Hepatic steatosis observed in both JAK2-deficient lines was not only a result of ectopic FA uptake but also resulted from enhanced expression of key enzymes involved in *de novo* lipogenesis. Lipogenic proteins like fatty acid synthase (FAS), stearoyl-CoA desaturase (SCD) 1, and peroxisome proliferator-activated receptor gamma (PPAR$\gamma$) were significantly upregulated as verified with Western blot quantification in both JAK2-deficient lines (Fig. 2b,c). Protein levels of PPAR$\alpha$, a major regulator of catabolism of FAs, were not changed in JAK2-deficient livers (Fig. 2b,c). In addition, detailed profiling of steatotic livers at 12 and 40 weeks of age revealed increased total FA and TG amounts characterised by significantly elevated unsaturated FAs like palmitoleic acid and oleic acid (Fig. 2d,e; Supplementary Fig. S2a–c). Similar results have been described for $GH^{tg}STAT5^{\Delta hep}$ mice where profound steatosis was a result of increased WAT mobilisation and the induction of hepatic *de novo* lipogenesis[24]. Collectively, these data indicate that a combination of increased mobilisation of WAT and the induction of hepatic *de novo* lipogenesis contributes to the steatotic phenotype of both JAK2-deficient lines.

**Liver tumourigenesis is delayed upon loss of JAK2 in $GH^{tg}$ mice.** High systemic levels of GH significantly reduce the life expectancy of $GH^{tg}$ mice[24,29] which is corrected upon hepatic STAT5[24] or JAK2 deficiency (Fig. 3a). We and others reported that hepatic STAT5 deficiency promotes liver tumour development and progression[22–24]. At 28 weeks of age, all $GH^{tg}STAT5^{\Delta hep}$ animals succumbed to liver tumours, which were characterised by broadening of liver cell cords and the loss of lobular plate architecture, pronounced cellular pleomorphisms and solid or trabecular growth pattern[24]. In contrast, $GH^{tg}$ mice developed first tumours 12 weeks later with an incidence rate of 34% (Fig. 3b,c). At this time point 100% of $GH^{tg}JAK2^{\Delta hep}$ and $JAK2^{\Delta hep}$ livers remained tumour-free (Fig. 3b,c), despite similar proliferation rates of hepatocytes (Supplementary Fig. S3a). The occurrence of liver tumours in $GH^{tg}JAK2^{\Delta hep}$ and $JAK2^{\Delta hep}$ mice was observed 5 months later with an incidence of 76% and 68%, respectively. Histopathological analysis revealed that $GH^{tg}JAK2^{\Delta hep}$ and $JAK2^{\Delta hep}$ tumours both displayed cellular

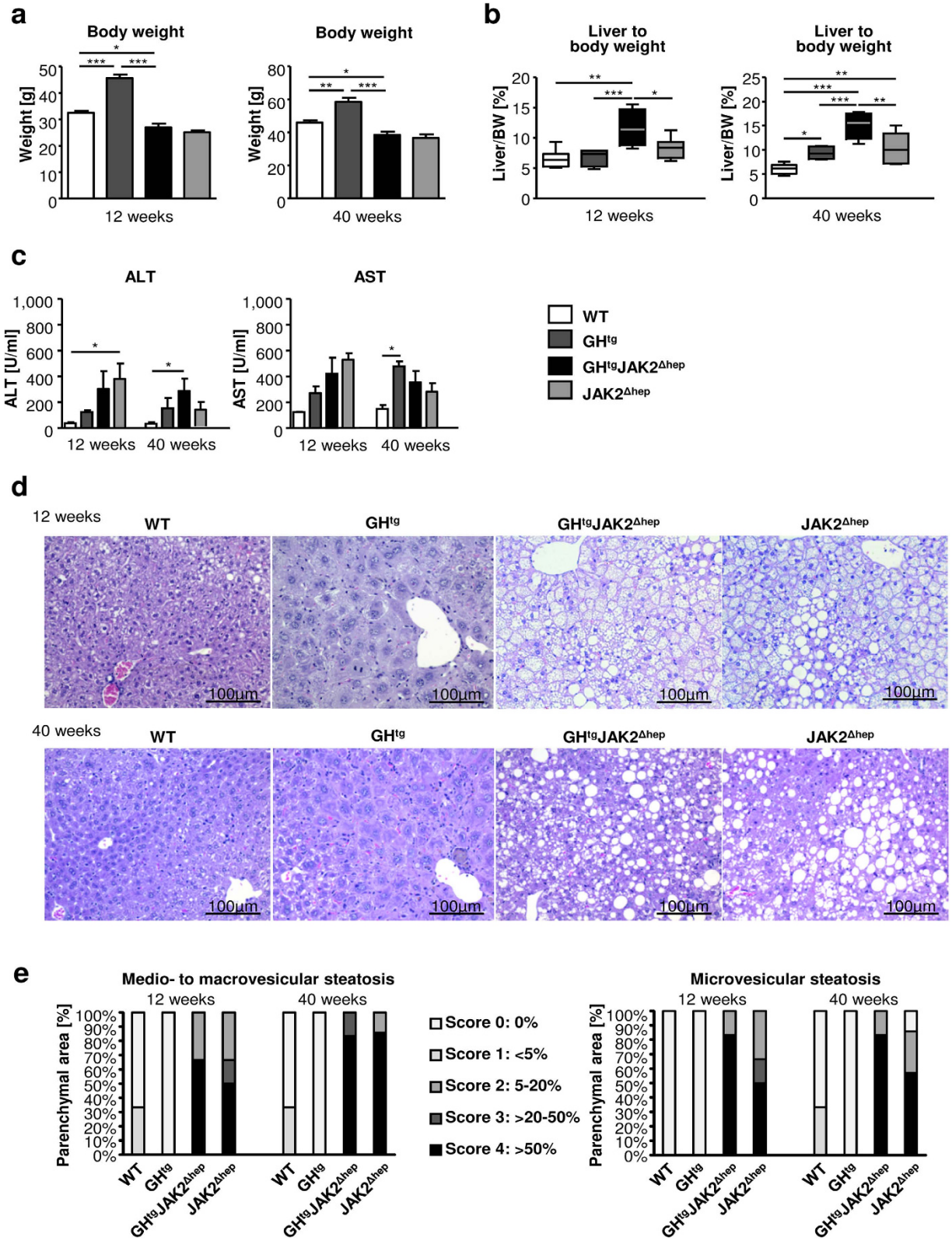



**Figure 1. Loss of hepatic JAK2 leads to profound hepatic steatosis.** (**a**) Body weights of mice at 12 and 40 weeks of age ($n \geq 4$/genotype for each time point) (**b**) Liver weight (LW)/body weight (BW) ratio of mutant and WT mice at indicated time points ($n \geq 4$/genotype). (**c**) Liver damage was quantified by measuring serum levels of the liver enzymes ALT and AST at indicated time points ($n \geq 4$/genotype). (**d**) H&E staining of liver sections at indicated time points. (**e**) Histopathological analysis assessing medio- and microvesicular steatosis ($n \geq 4$/genotype). *$p < 0.05$, **$p < 0.01$ and ***$p < 0.001$.

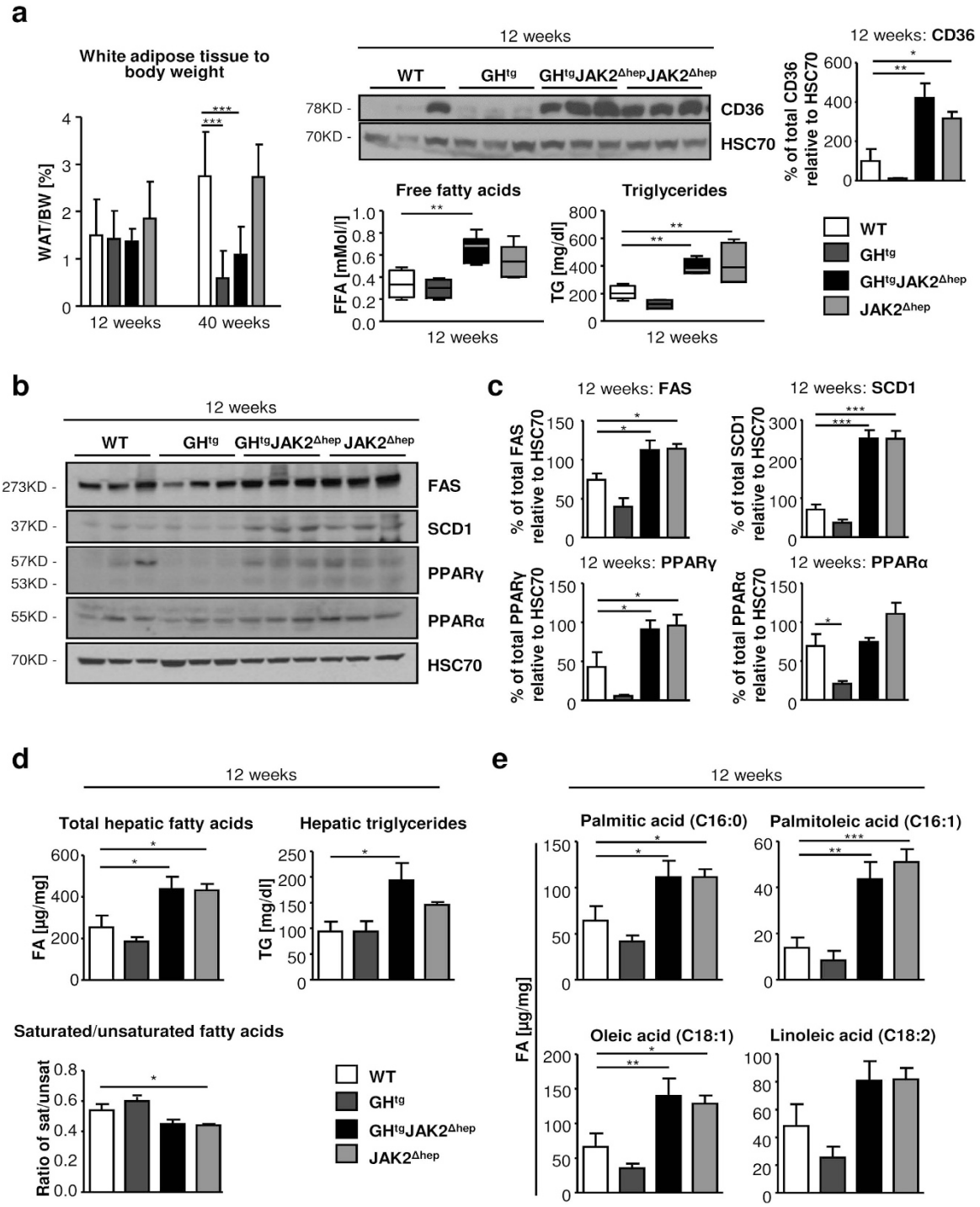



**Figure 2. JAK2 deficiency leads to increased mobilisation of fatty acids from the periphery and hepatic *de novo* lipogenesis.** (**a**) WAT/body weight ratio of perigonadal fat tissue indicating lipid mobilisation at indicated time points ($n \geq 4$/genotype). Representative Western blot analysis of whole liver homogenates and Western blot quantification of CD36 from 12-week-old animals. HSC70 is shown as loading control ($n = 3$/genotype). Scans of blots are presented in Supplementary Fig. S8. At 12 weeks of age, FFA serum levels, which were determined using an enzymatic test, were elevated in all mice lacking JAK2 ($n \geq 5$/genotype). Serum TG levels were measured at 12 weeks of age ($n \geq 4$/genotype). (**b**) Representative Western blot analysis of whole liver homogenates from 12-week-old animals. As a loading control HSC70 is shown ($n = 3$/genotype). (**c**) Western blot quantification of total FAS, SCD1, PPARγ and PPARα. Scans of blots are presented in Supplementary Fig. S8. (**d**) Hepatic total FA and TG amounts were measured at 12 weeks of age ($n \geq 6$/genotype). Ratio of saturated/unsaturated hepatic FAs at 12 weeks of age ($n \geq 8$/genotype). (**e**) Detailed profiling of steatotic livers using gas chromatography–mass spectrometry (GC-MS) showed elevated unsaturated FAs at 12 weeks of age ($n \geq 8$/genotype). $^{*}p < 0.05$, $^{**}p < 0.01$ and $^{***}p < 0.001$.

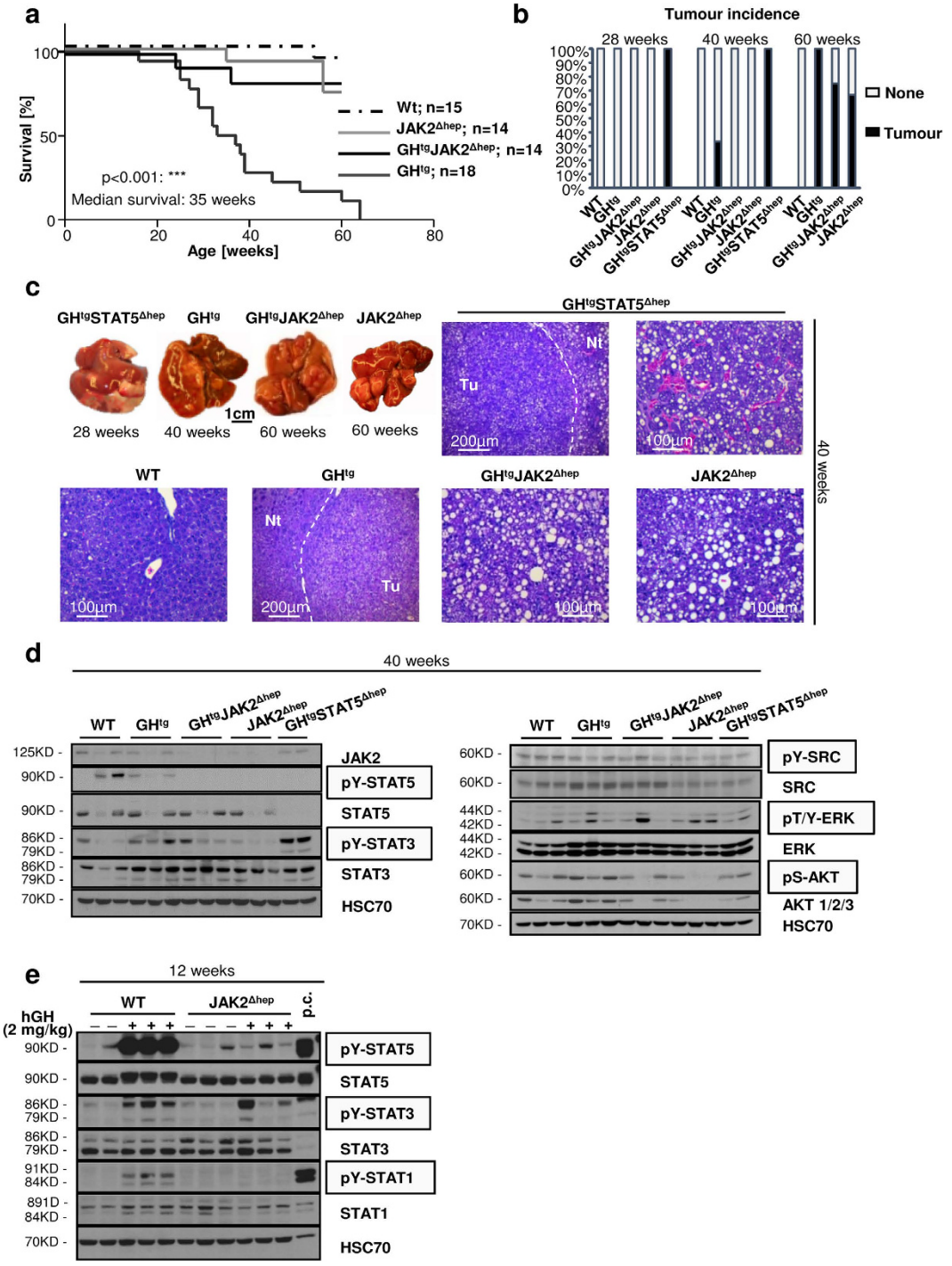



**Figure 3. Liver tumourigenesis is enhanced in STAT5-deficient animals, but diminished upon loss of its upstream kinase JAK2.** (**a**) Kaplan-Meier plot of male mice of four distinct genotypes over a time period of 60 weeks ($n \geq 14$/genotype). (**b**) Tumour incidence of livers of $GH^{tg}STAT5^{\Delta hep}$, $GH^{tg}$, $GH^{tg}JAK2^{\Delta hep}$ and $JAK2^{\Delta hep}$ mice. At 40 weeks of age, $GH^{tg}$ mice developed first liver tumours. Additional deletion of STAT5 in hepatocytes led to earlier and malignant tumours, whereas deletion of JAK2 resulted in delayed tumour formation at 60 weeks of age ($n \geq 4$/genotype). (**c**) Macroscopic appearance of tumourigenic livers at indicated time points. At 40 weeks, $GH^{tg}STAT5^{\Delta hep}$ mice had large steatotic and solid tumours. Tumours displayed a solid or trabecular growth pattern ($n \geq 4$/genotype). (**d**) Representative Western blot analysis of oncogenic signalling pathways in whole liver homogenates at 40 weeks of age. HSC70 is shown as loading control ($n \geq 2$/genotype). Scans of blots are presented in Supplementary Fig. S9. (**e**) Representative Western blot analysis of STAT proteins. As a loading control HSC70 is shown. WT and $JAK2^{\Delta hep}$ animals were injected intraperitoneally with vehicle or 2 mg/kg hGH and sacrificed 30 minutes thereafter ($n = 3$/treatment). Scans of blots and different exposure times of pY-STAT5 are presented in Supplementary Fig. S9. ***$p < 0.001$.

polymorphism and expression of markers for hepatocellular malignancy, such as oval cell fraction, and eosinophilic inclusions (Supplementary Fig. S3b).

Aberrant GH-mediated activation of STAT3 contributes to liver tumourigenesis in STAT5-deficient mice[19,20,24], which was clearly prevented in JAK2-deficient livers (Fig. 3d). In agreement, GH treatment of JAK2$^{\Delta hep}$ mice did not result in activation of STAT1/3/5 (Fig. 3e). Notably, not all GHR responsive signalling pathways require JAK2 activity[30]; these include GH dependent activation of SRC and ERK1/2, both of which can exert oncogenic functions in liver. However, neither SRC nor ERK1/2 was aberrantly activated in livers of GH$^{tg}$JAK2$^{\Delta hep}$ and GH$^{tg}$STAT5$^{\Delta hep}$ mice (Fig. 3d), suggesting that these signalling pathways do not contribute to liver tumourigenesis in either model. These results demonstrate that hepatic JAK2 deficiency - in contrast to STAT5 deletion - delays tumour formation in the GH transgenic background.

**Loss of JAK2 protects against ROS-induced oxidative damage.** Oxidative stress is a common feature of NAFLD and the resulting cellular damage (i.e. lipid peroxidation, protein oxidation and DNA damage)[8] contributes to liver tumourigenesis. To investigate the contribution of oxidative stress to progression of steatosis upon hepatic JAK2 or STAT5 deficiency, we determined ROS production within hepatocytes in 12-week-old animals by using different dyes, which are sensitive to mitochondrial membrane potential, mitochondrial or cytoplasmic ROS. For this purpose liver tissues were freshly excised, sectioned and subsequently stained. Mitochondrial membrane potential was similar among the genotypes, while mitochondrial and cytoplasmic ROS was increased in hepatocytes of steatotic GH$^{tg}$STAT5$^{\Delta hep}$, GH$^{tg}$JAK2$^{\Delta hep}$ and JAK2$^{\Delta hep}$ livers (Fig. 4a, Supplementary Fig. S4a). Cytoplasmic ROS in GH$^{tg}$JAK2$^{\Delta hep}$, JAK2$^{\Delta hep}$ and GH$^{tg}$STAT5$^{\Delta hep}$ livers was recognised as small subcellular structures indicative for peroxisome activation. Surprisingly, despite similarly elevated ROS levels, increased DNA damage (pH2AX), protein carbonylation (indicative for protein oxidation), and malondialdehyde (MDA), a side product of lipid peroxidation, were only significantly increased in GH$^{tg}$STAT5$^{\Delta hep}$ and GH$^{tg}$ animals at 12 and 40 weeks of age (Fig. 4b,c; Supplementary Fig. S4b,c). These data indicate that hepatic JAK2 deficiency protects against ROS-induced DNA damage and oxidation of lipids and proteins, while STAT5 deficiency results in accelerated oxidative damage.

**Loss of JAK2 leads to increased detoxification by glutathione S-transferases.** Protection from ROS-mediated oxidative damage is conducted by several defence mechanisms, such as ROS clearance and the detoxification machinery[9]. Inadequate defence mechanisms result in cell damage and thereby, increase the risk for malignant transformation (Fig. 5a). Thus, to define the mechanisms underlying the different degrees of oxidative damage upon hepatic JAK2 or STAT5 deficiency, we examined the expression levels of enzymes involved in ROS clearance and detoxification. Global gene-expression analysis of enzymes governing ROS clearance revealed that the expression of superoxide dismutase 3 (*Sod3*), glutathione peroxidase 2 (*Gpx2*), *Gpx3* and *Gpx7* was highly upregulated in GH$^{tg}$ animals at 12 weeks of age (Fig. 5b,c; Supplementary Fig. S5a). SOD3, GPX2 and GPX3 execute extracellular functions and have been shown to exert anti-inflammatory effects[31,32]. However, expression levels were not altered in steatotic GH$^{tg}$STAT5$^{\Delta hep}$, GH$^{tg}$JAK2$^{\Delta hep}$ and JAK2$^{\Delta hep}$ livers compared to WT littermates. The second major antioxidant defence mechanism is executed by glutathione-S transferases (GST), which directly detoxify oxidized macromolecules to prevent cell damage (Fig. 5a). At 12 and 40 weeks of age, Affymetrix and qRT-PCR analyses of whole liver extracts revealed strong upregulation of *Gsta1*, *Gsta2* and *Gstm3* particularly in JAK2-deficient livers (Fig. 5c,d; Supplementary Fig. S5b,c). Additionally, the expression of glutathione synthetase (*GSS*), which is necessary for glutathione biosynthesis and GST functionality, was increased in GH$^{tg}$JAK2$^{\Delta hep}$ and JAK2$^{\Delta hep}$ mice (Fig. 5d). In line, protein levels of GSTA1/2 and GST activity were significantly elevated in GH$^{tg}$JAK2$^{\Delta hep}$ and JAK2$^{\Delta hep}$ livers (Fig. 5e,f; Supplementary Fig. S5d). Taken together, these results suggest that loss of hepatic JAK2 diminishes ROS-induced oxidative damage through increased expression and activity of GST enzymes.

**Pharmacological inhibition and siRNA-mediated knockdown of *Jak2* leads to increased expression of *Gst* isoforms and reduced DNA damage.** To verify that loss of JAK2 activity directly accounted for the induction of *Gst* expression, we treated WT littermates with the JAK inhibitor ruxolitinib for 2 days. Ruxolitinib treatment induced strong expression of *Gsta1*, *Gsta2* and *Gstm3*, resembling the hepatic knockout of *Jak2*. Liver sections exhibited normal liver architecture in ruxolitinib-treated mice (Fig. 6a; Supplementary Fig. S6a). To assess whether *Gst* expression was hepatocyte-specific, we made use of immortalised murine p19$^{ARF-/-}$ hepatocytes[33], which were characterised by formation of monolayers, retention of morphological features and the expression of hepatocyte-specific markers as verified by Western blotting (Supplementary Fig. S6b). p19$^{ARF-/-}$ hepatocytes were responsive to GH as indicated by STAT5 activation (Fig. 6b) and JAK2-STAT5 signalling could be completely inhibited by ruxolitinib treatment (Fig. 6c). Importantly, already after 6 hours of JAK2 inhibition, p19$^{ARF-/-}$ hepatocytes displayed increased *Gsta1*, *Gsta2* and *Gstm3* expression (Fig. 6d).

Next, we set out to functionally verify, if inhibition of JAK2 by ruxolitinib would reduce oxidative damage. We generated ROS-induced DNA damage in p19$^{ARF-/-}$ hepatocytes by $H_2O_2$ exposure. Indeed, pre-treatment with ruxolitinib led to a significant reduction of pH2AX expression in hepatocytes (Supplementary Fig. S6c). Similarly, pre-treatment of p19$^{ARF-/-}$ hepatocytes with ruxolitinib resulted in a pronounced reduction of pH2AX expression in hepatocytes upon palmitic acid (PA)-induced lipotoxicity (Fig. 6e)[34]. To exclude potential JAK2 independent effects of ruxolitinib treatment, we additionally made use of small interfering (si)RNA-mediated knockdown of *Jak2*. Complete knockdown in p19$^{ARF-/-}$ hepatocytes was accomplished after 48 hours (Fig. 6f). In accordance with ruxolitinib-treated p19$^{ARF-/-}$ hepatocytes, knockdown of *Jak2* resulted in increased *Gsta1*, *Gsta2* and *Gstm3* expression (Fig. 6g) and reduced ROS-induced DNA-damage after $H_2O_2$ and PA exposure (Fig. 6h; Supplementary Fig. S6d).

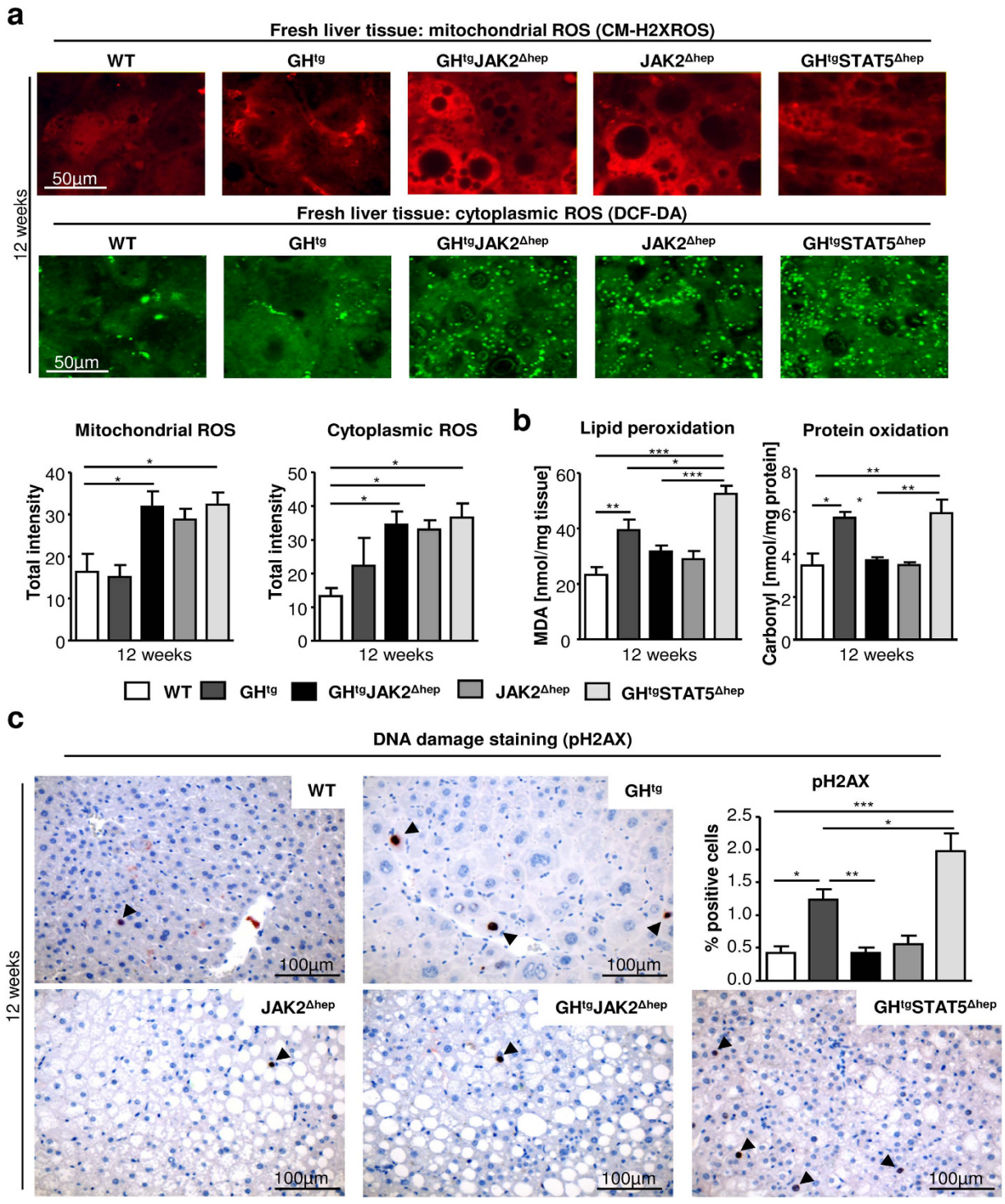



**Figure 4. Hepatic JAK2 deficiency protects against ROS-induced lipid peroxidation, protein oxidation and DNA damage.** (**a**) Freshly cut livers were stained with fluorescent dyes sensitive to mitochondrial and cytoplasmic ROS. Imaging was performed with an inverted confocal microscope ($n \geq 5$/genotype). (**b**) Lipid peroxidation was assessed by measuring its by-product malondialdehyde (MDA) at 12 weeks of age. Measurement of protein oxidation was performed using colorimetric assay ($n \geq 5$/genotype). (**c**) Representative liver sections of 12-week-old mice stained with antibodies against phosphorylated H2AX to detect DNA damage. Quantification of positive hepatocytes by image analysis ($n \geq 5$/genotype). *$p < 0.05$, **$p < 0.01$ and ***$p < 0.001$.

Thus, in agreement with genetic loss of JAK2, these data imply that pharmacological inhibition and siNRA-mediated knockdown of *Jak2* reduces oxidative stress-induced DNA damage, presumably, through upregulation of *Gst* enzymes.

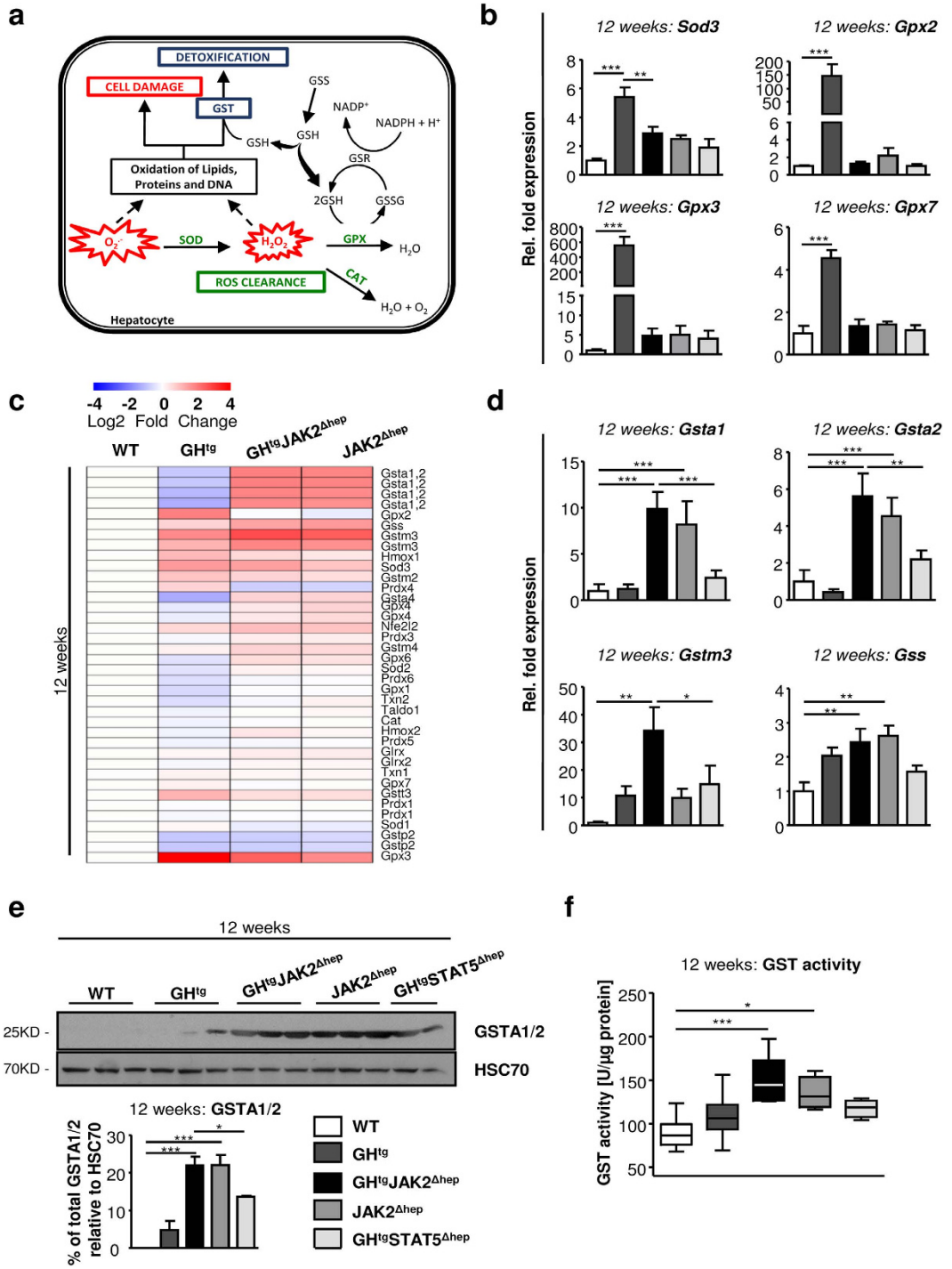



**Figure 5. Genetic deletion of hepatic *Jak2* results in increased expression and activity of detoxifying enzymes.** (**a**) Schematic overview of the antioxidative defence system. SOD, CAT and GPX are the primary antioxidant enzymes which inactivate ROS into intermediates. GST catalyses the conjugation of the reduced form of GSH to oxidised products to detoxify oxidised lipids, proteins and DNA ($H^+$: hydrogen ion, SOD: superoxide dismutase, CAT: catalase, GPX: glutathione peroxidase, GSSG: oxidized glutathione, GSH: glutathione, GSS: glutathione synthetase, GSR: glutathione reductase, GST: glutathione S-transferase). (**b**) By means of qRT-PCR, mRNA levels of *Sod3*, *Gpx2*, *Gpx3* and *Gpx7* involved in antioxidant response were measured in livers at 12 weeks of age (n = 6/genotype). Ct values were normalised to *Gapdh* and *Rpl12a*. (**c**) At 12 weeks of age transcriptome analysis of genes coding for enzymes involved in antioxidant defence. (**d**) mRNA expression levels of *Gsta1*, *Gsta2*, *Gstm3* and *Gss* at 12 weeks of age (n = 6/genotype). Ct values were normalised to *Gapdh*. (**e**) Representative Western blot analysis of whole liver homogenates and Western blot quantification of GSTA1/2 from 12-week-old animals. As a loading control HSC70 is shown (n ≥ 2/genotype). Scans of blots are presented in Supplementary Fig. S10. (**f**) GST activity was assessed in livers from 12-week-old mice using a colorimetric assay (n ≥ 6/genotype). *$p < 0.05$, **$p < 0.01$ and ***$p < 0.001$.

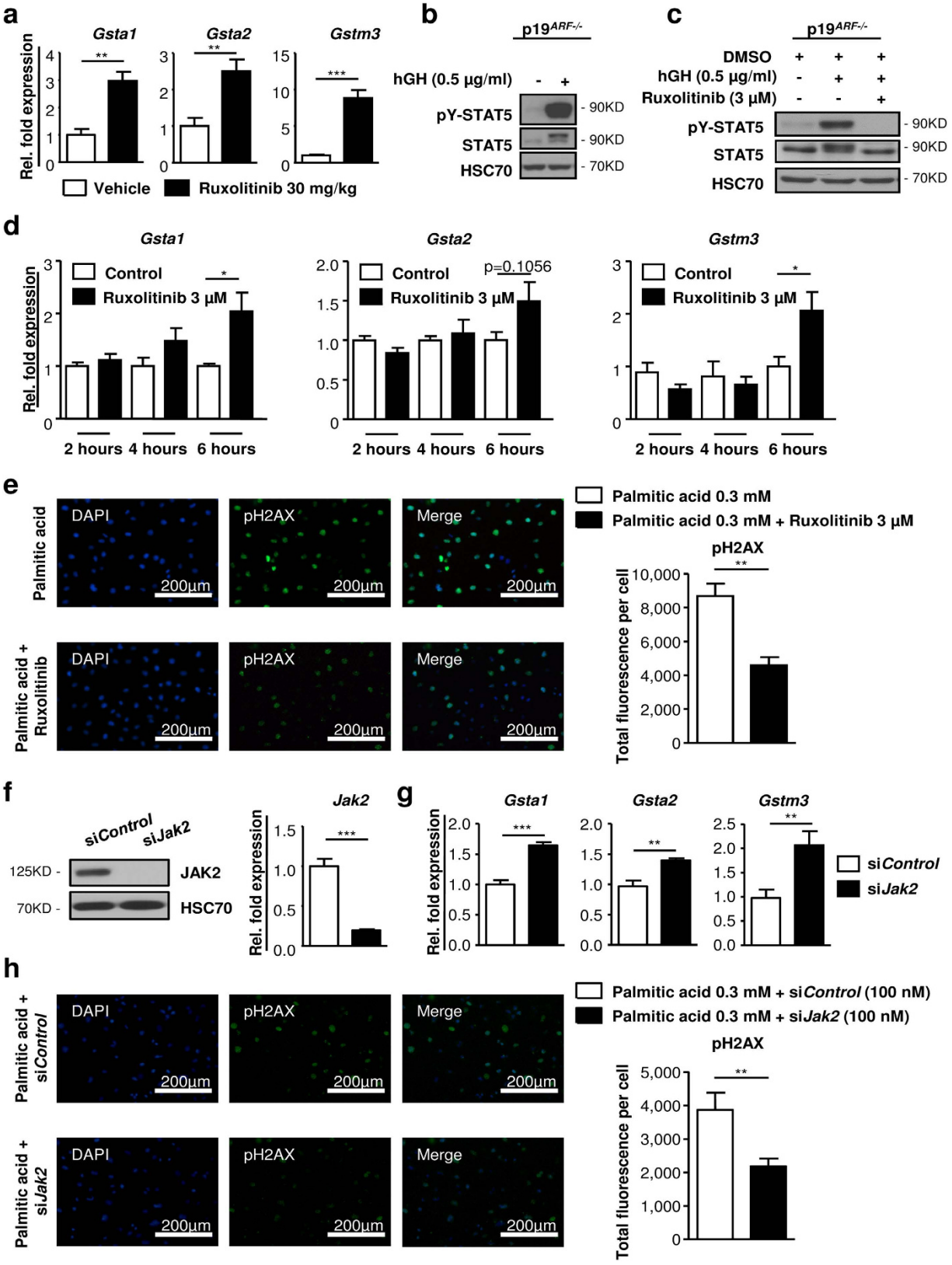



**Figure 6. Pharmacological inhibition and siRNA-mediated knockdown of *Jak2* induces expression of *Gst* isoforms and reduces DNA damage upon oxidative stress.** (**a**) Control littermates not expressing the AlfpCre were treated with vehicle or 30 mg/kg ruxolitinib twice daily for 2 days by oral gavage (n = 4/treatment). mRNA expression levels of *Gsta1*, *Gsta2* and *Gstm3* upon ruxolitinib treatment. Ct values were normalised to *Gapdh*. (**b**) Representative Western blot analysis showed activation of STAT5 in immortalised $p19^{ARF-/-}$ hepatocytes upon human GH stimulation (0.5 µg/ml). Prior to stimulation, hepatocytes were starved for 2 hours (1% FCS and without growth factors). As a loading control HSC70 is shown (n = 3 independent experiments). Scans of

blots are presented in Supplementary Fig. S11. (**c**) After treatment with 3 μM ruxolitinib for 24 hours, $p19^{ARF-/-}$ hepatocytes were stimulated with 0.5 μg/ml of human GH and analysed by Western blotting. As a loading control HSC70 is shown (n = 3 independent experiments). Scans of blots are presented in Supplementary Fig. S11. (**d**) $p19^{ARF-/-}$ hepatocytes were treated with 3 μM ruxolitinib without hGH for indicated time points. mRNA expression levels of *Gsta1*, *Gsta2* and *Gstm3* were measured. Results are shown from three independent experiments. Ct values were normalised to *Gapdh*. (**e**) Immunofluorescence staining of DAPI (blue) and phosphorylated H2AX (green). $p19^{ARF-/-}$ hepatocytes were pre-treated 24 hours with ruxolitinib or DMSO. Cells were exposed with 0.3 mM palmitic acid (PA) for another 24 hours containing either ruxolitinib or DMSO. Fluorescence intensity was quantified by image analysis (n = 3 independent experiments). (**f**) $p19^{ARF-/-}$ hepatocytes were transfected with non-targeting siRNA (si*Control*) or siRNA against *Jak2* (si*Jak2*) for 48 hours. Representative Western blot analysis and mRNA expression levels showed efficient knockdown in $p19^{ARF-/-}$ hepatocytes. As a loading control HSC70 is shown. Scans of blots are presented in Supplementary Fig. S11. (**g**) $p19^{ARF-/-}$ hepatocytes were transfected with si*Jak2* or si*Control* for 48 hours. mRNA expression levels of *Gsta1*, *Gsta2* and *Gstm3* upon siRNA-mediated knockdown were measured. Ct values were normalised to *Gapdh*. (**h**) Immunofluorescence staining of DAPI (blue) and phosphorylated H2AX (green). $p19^{ARF-/-}$ hepatocytes were pre-treated 48 hours with si*Jak2* or si*Control*. Cells were exposed with 0.3 mM PA for another 24 hours. Fluorescence intensity was quantified by image analysis (n = 2 independent experiments). $^{*}p < 0.05$, $^{**}p < 0.01$ and $^{***}p < 0.001$.

Collectively, our data suggest that STAT5 deficiency aggravates liver tumourigenesis in the $GH^{tg}$ background due to aberrant STAT3 activation and increased oxidative damage. In contrast, JAK2 deficiency delays tumour formation in $GH^{tg}$ mice, which is linked to insignificant oncogenic STAT3 signalling and reduced ROS-induced oxidative damage. Our conclusion model (Supplementary Fig. S7) depicts the surprising difference between hepatic STAT5 and JAK2 deficiency with consequence for oxidative liver damage.

## Discussion

Development of NAFLD has been associated with impaired GH signalling[14,15]. Mouse models have further linked loss of GH signalling to NAFLD by demonstrating that liver-specific deficiency of GHR, JAK2 or STAT5 results in metabolic defects, which manifest in hepatic steatosis[17–19]. HCC is a common consequence of chronic liver disease[4,5]. While JAK2-STAT5 signalling exerts oncogenic functions in hematopoietic cancers[35], GH-activated STAT5 has a protective role in mouse models of chronic liver disease[12,20,22–24,36].

Here, we describe that hepatic JAK2 deficiency protects against oxidative liver damage and thereby, potentially reduces the risk for liver tumourigenesis in a $GH^{tg}$ mouse model.

We confirm that loss of JAK2 leads to overt hepatomegaly and steatosis. This phenotype was described to depend on GH-dependent mobilisation of FFAs from WAT and their increased hepatic uptake mediated by elevated expression of PPARγ and CD36[18,27]. In contrast to $GH^{tg}JAK2^{\Delta hep}$ mice, $JAK2^{\Delta hep}$ animals did not display strong increases in circulating FFAs and a depletion of WAT stores. However, even in presence of normal circulating FFA concentrations, transgenic CD36 overexpression in murine liver results in markedly elevated FA uptake and lipid storage[37]. Thus, the greatly increased CD36 expression in $JAK2^{\Delta hep}$ livers likely promotes hepatic FA uptake and deposition in a similar manner. CD36 is a transcriptional target of PPARγ[38] and previous work links GH signalling to transcriptional repression of PPARγ[18]. Accordingly, hyperactivated GH signalling, as seen in $GH^{tg}$ mice, suppresses the transcription of PPARγ and its downstream targets, CD36 and SCD1[39]. Conversely, disruption of GH signalling by hepatic deletion of JAK2 or STAT5 results in increased expression of *Cd36*[18,19], which we additionally confirmed by knockdown of *Jak2* in $p19^{ARF-/-}$ hepatocytes (Supplementary Fig. S6e). We extend these findings by demonstrating that hepatic JAK2 deficiency results in elevated protein expression of the lipogenic enzymes FAS and SCD1, both of which are frequently linked to NAFLD[40,41]. In agreement with the upregulation of FAS and SCD1[40,41], a specific increase in palmitate (C16:0), palmitoleate (C16:1) and oleate (C18:1) concentrations was observed, suggesting elevated *de novo* synthesis and conversion of saturated FAs into monounsaturated FAs.

A characteristic feature of NAFLD is an increased formation of ROS. Increases in hepatic FA species significantly contribute to ROS production by oxidative events[7] and thereby to lipotoxicity[42]. Persistent oxidative stress adds to chronic liver injury and this amplifies the risk to develop liver cancer[7]. In line, disruption of GHR-JAK2-STAT5 signalling results in increased production of cytoplasmic and mitochondrial ROS in steatotic hepatocytes[20]. However, despite similar degrees of fatty degeneration and ROS production in $GH^{tg}STAT5^{\Delta hep}$ and $GH^{tg}JAK2^{\Delta hep}$ livers, hepatic JAK2 deficiency delayed tumour formation in the $GH^{tg}$ background. In accordance with our data, increased activation of JAK2 correlates with poor overall survival in HCC patients with high circulating prolactin levels[43]. Furthermore, mice lacking the GHR in a model of cholestasis were largely resistant to tumour development despite an aggravation of liver fibrosis[44], while a clinical study revealed very low incidence of cancer in a population suffering from a *GHR* mutation[45]. Besides the clinically approved ruxolitinib, there are more than 10 distinct JAK2 inhibitors in clinical trials[46] emphasising the pharmacological relevance of this pathway.

Aberrant GH-mediated activation of STAT3 was associated with accelerated liver tumourigenesis of STAT5-deficient livers[19,20,24]. In agreement with the requirement of JAK2 for GH-mediated activation of STAT proteins[30], excessive STAT3 activity was not observed in JAK2-deficient livers and thus presumably contributed to delayed tumour onset in $GH^{tg}JAK2^{\Delta hep}$ mice. Intriguingly, in the absence of JAK2, elevated ROS accumulation did not correlate with augmented lipid peroxidation, protein oxidation and DNA damage. Several potential therapeutic strategies to lower oxidative stress in NAFLD have been suggested[10]. In particular, vitamin E supplementation is used to decrease TG accumulation and to lower lipid peroxidation[10,47]. Along this line, we show that JAK2 deficiency led to increased expression and activity of GSTs, a group of detoxification enzymes involved in protection

against oxidative stress[48]. A similar increase in GST expression and activity was not detectable in STAT5-deficient livers, in which elevated ROS accumulation correlated with augmented oxidative damage. A recent study linked STAT5 activation to increased ROS production in chronic myeloid leukaemia cells by repressing antioxidant enzymes suggesting tissue-specific functions of STAT5[49].

In support of our *in vivo* findings, treatment of $p19^{ARF-/-}$ hepatocytes with ruxolitinib and siRNA against *Jak2* not only resulted in *Gst* upregulation, but was also efficient in reducing $H_2O_2$ and palmitic acid induced oxidative DNA damage. Given the detoxifying role of GST isoforms upregulation in the absence of JAK2 potentially contributes to decreased oxidative damage and delayed tumour initiation in $GH^{tg}JAK2^{\Delta hep}$ mice. The role of GSTs in NAFLD and its progression are not understood. However, a *GSTM1-null* genotype has been implicated in NAFLD development and this finding might be correlated with increased HCC risk in the Asian population[50]. GST activity was further reported to decrease with NAFLD progression accompanied by a reduced pool of glutathione, which inversely correlated with lipid peroxidation[11]. In conjunction, our findings provide evidence that GST enzymes - through resolution of oxidative stress - might be beneficial for the prevention of NAFLD-associated liver damage.

The expression of *Gsts* has been shown to be induced by nuclear factor-like 2 (NRF2), and the nuclear hormone receptors retinoic acid receptor alpha (RARα) and retinoid X receptor alpha (RXRα)[51]. Neither *Nrf2* mRNA expression nor protein levels of RARα and RXRα were significantly upregulated in JAK2-deficient livers (Supplementary Fig. S5e). Interestingly, JAK2 can exert nuclear or peri-nuclear function in hepatocytes, mammary epithelial or hematologic cells[52–54]. This might be a possible mechanism to repress *Gst* induction in the presence of JAK2. However, JAK2-dependent regulation of chromatin architecture identified to date is rather associated with activating than repressive function[52].

Collectively, we show that ROS-mediated oxidative damage is prevented in steatotic JAK2 deficient livers, which correlates with delayed tumour onset in the $GH^{tg}$ background. Importantly, in line with findings from the genetic model, our data indicate that pharmacologic JAK2 inhibition protects against oxidative damage. Further studies assessing the effectiveness of JAK2 inhibitors to lower oxidative stress may provide a rationale for the potential use in chronic liver disease.

## Methods

**Mice.** Mice with hepatic deletion of *Jak2* or *Stat5* (*Jak2*$^{fl/fl}$[25], *Stat5ab*$^{fl/fl}$; referred to as $JAK2^{\Delta hep}$ or $STAT5^{\Delta hep}$[55]) were bred with GH transgenic animals ($GH^{tg}$; described in ref. 26) to generate $GH^{tg}JAK2^{\Delta hep}$ and $GH^{tg}STAT5^{\Delta hep}$ mice, respectively. Littermates not expressing AlfpCre recombinase served as WT controls. The genetic background of all mice analysed was C57BL/6J × SV129. For all analyses only male mice were used. Animal experiments were performed according to an ethical animal license protocol approved by the authorities of the Austrian government and the Medical University of Vienna. Maintenance and experimental procedures of mice are described in detail in the Supplementary materials and methods (see Supplementary information).

**Serum biochemistry.** Serum levels of alanine aminotransferase (ALT) and aspartate-aminotransferase (AST) were determined using the test strip-based Reflotron Plus analyser (Roche). Free fatty acid levels were assessed photometrically using the NEFA-HR(2) kit (Wako).

**Measurement of hepatic metabolites.** Hepatic triglycerides (CaymanChemical), lipid peroxidation, protein oxidation and GST activity (BioVision) were determined using commercially available colorimetric assays. The measurement of ROS levels and hepatic fatty acid is described in Supplementary materials and methods (see Supplementary information).

**Immunoblotting and immunohistochemistry.** Western blot analyses and immunohistochemistry were performed according to standard protocols. Antibodies used are listed in detail in the Supplementary materials and methods (see Supplementary information).

**Microarray analysis.** At 12 and 40 weeks, total RNA from 3 livers/genotype (WT, $GH^{tg}$, $GH^{tg}JAK2^{\Delta hep}$ and $JAK2^{\Delta hep}$) were isolated using the RNAeasy Kit (#74104; Quiagen) and hybridised to GeneChip Mouse Gene 1.0 ST array (Affymetrix). Microarray data and description of the experimental design is deposited under ArrayExpress, with the accession number: E-MTAB-3774. The detailed analysis is provided in the Supplementary materials and methods (see Supplementary information).

**Analysis of gene expression by quantitative PCR.** Total RNA was isolated with TRIzol reagent (Invitrogen) and reverse transcribed using Revert Aid cDNA synthesis kit (Thermo Fisher Scientific). The detailed method together with the primer sequences is provided in the Supplementary materials and methods (see Supplementary information).

**Cell Culture.** Hepatocytes of $p19^{ARF-/-}$ mice were isolated and propagated as described[33]. Maintenance of $p19^{ARF-/-}$ hepatocytes and *in vitro* experiments are described in the Supplementary materials and methods (see Supplementary information).

**Statistics.** All values are represented as means ± standard error of the mean if not indicated otherwise. Statistical significance was evaluated using a confidence interval of 95% with either one-way ANOVA followed by Tukey's, Dunns' or Bonferroni's post-hoc test for multiple comparison or two-tailed student's t-test for the comparison of two groups. Differences between experimental groups were considered significant at $^{*}p < 0.05$, $^{**}p < 0.01$ and $^{***}p < 0.001$. All calculations were performed using GraphPad Prism software (La Jolla, CA).

## References


1. Duan, X. F., Tang, P., Li, Q. & Yu, Z. T. Obesity, adipokines and hepatocellular carcinoma. *Int J Cancer* **133,** 1776–1783, doi: 10.1002/ijc.28105 (2013).
2. Baffy, G., Brunt, E. M. & Caldwell, S. H. Hepatocellular carcinoma in non-alcoholic fatty liver disease: an emerging menace. *J Hepatol.* **56,** 1384–1391, doi: 10.1016/j.jhep.2011.10.027 (2012).
3. Stojsavljevic, S., Gomercic Palcic, M., Virovic Jukic, L., Smircic Duvnjak, L. & Duvnjak, M. Adipokines and proinflammatory cytokines, the key mediators in the pathogenesis of nonalcoholic fatty liver disease. *World J Gastroenterol.* **20,** 18070–18091, doi: 10.3748/wjg.v20.i48.18070 (2014).
4. Ertle, J. *et al.* Non-alcoholic fatty liver disease progresses to hepatocellular carcinoma in the absence of apparent cirrhosis. *Int J Cancer* **128,** 2436–2443, doi: 10.1002/ijc.25797 (2011).
5. Paradis, V. *et al.* Hepatocellular carcinomas in patients with metabolic syndrome often develop without significant liver fibrosis: a pathological analysis. *Hepatology* **49,** 851–859, doi: 10.1002/hep.22734 (2009).
6. Matsuzawa, N. *et al.* Lipid-induced oxidative stress causes steatohepatitis in mice fed an atherogenic diet. *Hepatology* **46,** 1392–1403, doi: 10.1002/hep.21874 (2007).
7. Paradies, G., Paradies, V., Ruggiero, F. M. & Petrosillo, G. Oxidative stress, cardiolipin and mitochondrial dysfunction in nonalcoholic fatty liver disease. *World J Gastroenterol.* **20,** 14205–14218, doi: 10.3748/wjg.v20.i39.14205 (2014).
8. Klaunig, J. E., Kamendulis, L. M. & Hocevar, B. A. Oxidative stress and oxidative damage in carcinogenesis. *Toxicol Pathol.* **38,** 96–109, doi: 10.1177/0192623309356453 (2010).
9. Liu, W., Baker, S. S., Baker, R. D. & Zhu, L. Antioxidant Mechanisms in Nonalcoholic Fatty Liver Disease. *Curr Drug Targets* (2015).
10. Polimeni, L. *et al.* Oxidative stress: New insights on the association of non-alcoholic fatty liver disease and atherosclerosis. *World J Hepatol.* **7,** 1325–1336, doi: 10.4254/wjh.v7.i10.1325 (2015).
11. Hardwick, R. N., Fisher, C. D., Canet, M. J., Lake, A. D. & Cherrington, N. J. Diversity in antioxidant response enzymes in progressive stages of human nonalcoholic fatty liver disease. *Drug Metab Dispos.* **38,** 2293–2301, doi: 10.1124/dmd.110.035006 (2010).
12. Baik, M., Yu, J. H. & Hennighausen, L. Growth hormone-STAT5 regulation of growth, hepatocellular carcinoma, and liver metabolism.*Ann N Y Acad Sci.* **1229,** 29–37, doi: 10.1111/j.1749-6632.2011.06100.x (2011).
13. Riordan, J. D. & Nadeau, J. H. Modeling progressive non-alcoholic fatty liver disease in the laboratory mouse. *Mamm Genome* **25,** 473–486, doi: 10.1007/s00335-014-9521-3 (2014).
14. Laron, Z., Ginsberg, S. & Webb, M. Nonalcoholic fatty liver in patients with Laron syndrome and GH gene deletion - preliminary report. *Growth hormone & IGF research : official journal of the Growth Hormone Research Society and the International IGF Research Society* **18,** 434–438, doi: 10.1016/j.ghir.2008.03.003 (2008).
15. Fusco, A. *et al.* Nonalcoholic fatty liver disease is associated with increased GHBP and reduced GH/IGF-I levels. *Clin Endocrinol* (*Oxf*) **77,** 531–536, doi: 10.1111/j.1365-2265.2011.04291.x (2012).
16. Mueller, K. M. *et al.* Hepatic growth hormone and glucocorticoid receptor signaling in body growth, steatosis and metabolic liver cancer development. *Molecular and cellular endocrinology* **361,** 1–11, doi: 10.1016/j.mce.2012.03.026 (2012).
17. Fan, Y. *et al.* Liver-specific deletion of the growth hormone receptor reveals essential role of growth hormone signaling in hepatic lipid metabolism. *The Journal of biological chemistry* **284,** 19937–19944, doi: 10.1074/jbc.M109.014308 (2009).
18. Sos, B. C. *et al.* Abrogation of growth hormone secretion rescues fatty liver in mice with hepatocyte-specific deletion of JAK2. *J Clin Invest* **121,** 1412–1423, doi: 42894 [pii] 10.1172/JCI42894 (2011).
19. Cui, Y. *et al.* Loss of signal transducer and activator of transcription 5 leads to hepatosteatosis and impaired liver regeneration. *Hepatology* **46,** 504–513, doi: 10.1002/hep.21713 (2007).
20. Mueller, K. M. *et al.* Impairment of hepatic growth hormone and glucocorticoid receptor signaling causes steatosis and hepatocellular carcinoma in mice. *Hepatology* **54,** 1398–1409, doi: 10.1002/hep.24509 (2011).
21. Shi, S. Y. *et al.* Hepatocyte-specific deletion of Janus kinase 2 (JAK2) protects against diet-induced steatohepatitis and glucose intolerance. *The Journal of biological chemistry* **287,** 10277–10288, doi: 10.1074/jbc.M111.317453 (2012).
22. Hosui, A. *et al.* Loss of STAT5 causes liver fibrosis and cancer development through increased TGF-{beta} and STAT3 activation. *J Exp Med.* **206,** 819–831, doi: jem.20080003 [pii] 10.1084/jem.20080003 (2009).
23. Yu, J. H., Zhu, B. M., Riedlinger, G., Kang, K. & Hennighausen, L. The liver-specific tumor suppressor STAT5 controls expression of the reactive oxygen species-generating enzyme NOX4 and the proapoptotic proteins PUMA and BIM in mice. *Hepatology* **56,** 2375–2386, doi: 10.1002/hep.25900 (2012).
24. Friedbichler, K. *et al.* Growth-hormone-induced signal transducer and activator of transcription 5 signaling causes gigantism, inflammation, and premature death but protects mice from aggressive liver cancer. *Hepatology* **55,** 941–952, doi: 10.1002/hep.24765 (2012).
25. Krempler, A. *et al.* Generation of a conditional knockout allele for the Janus kinase 2 (Jak2) gene in mice. *Genesis* **40,** 52–57, doi: 10.1002/gene.20063 (2004).
26. Snibson, K. J., Bhathal, P. S., Hardy, C. L., Brandon, M. R. & Adams, T. E. High, persistent hepatocellular proliferation and apoptosis precede hepatocarcinogenesis in growth hormone transgenic mice. *Liver* **19,** 242–252 (1999).
27. Nordstrom, S. M., Tran, J. L., Sos, B. C., Wagner, K. U. & Weiss, E. J. Disruption of JAK2 in adipocytes impairs lipolysis and improves fatty liver in mice with elevated GH. *Mol Endocrinol.* **27,** 1333–1342, doi: 10.1210/me.2013-1110 (2013).
28. Vollenweider, P., von Eckardstein, A. & Widmann, C. HDLs, diabetes, and metabolic syndrome. *Handb Exp Pharmacol* **224,** 405–421, doi: 10.1007/978-3-319-09665-0_12 (2015).
29. Wanke, R., Hermanns, W., Folger, S., Wolf, E. & Brem, G. Accelerated growth and visceral lesions in transgenic mice expressing foreign genes of the growth hormone family: an overview. *Pediatr Nephrol.* **5,** 513–521 (1991).
30. Barclay, J. L. *et al. In vivo* targeting of the growth hormone receptor (GHR) Box1 sequence demonstrates that the GHR does not signal exclusively through JAK2. *Mol Endocrinol.* **24,** 204–217, doi: 10.1210/me.2009-0233 (2010).
31. Laurila, J. P., Laatikainen, L. E., Castellone, M. D. & Laukkanen, M. O. SOD3 reduces inflammatory cell migration by regulating adhesion molecule and cytokine expression. *PloS one* **4,** e5786, doi: 10.1371/journal.pone.0005786 (2009).
32. Brigelius-Flohe, R. & Kipp, A. P. Physiological functions of GPx2 and its role in inflammation-triggered carcinogenesis.*Ann N Y Acad Sci.* **1259,** 19–25, doi: 10.1111/j.1749-6632.2012.06574.x (2012).
33. Mikula, M. *et al.* Immortalized p19ARF null hepatocytes restore liver injury and generate hepatic progenitors after transplantation. *Hepatology* **39,** 628–634, doi: 10.1002/hep.20084 (2004).
34. Wei, Y., Wang, D., Topczewski, F. & Pagliassotti, M. J. Saturated fatty acids induce endoplasmic reticulum stress and apoptosis independently of ceramide in liver cells. *Am J Physiol Endocrinol Metab* **291,** E275–E281, doi: 10.1152/ajpendo.00644.2005 (2006).
35. Valentino, L. & Pierre, J. JAK/STAT signal transduction: regulators and implication in hematological malignancies. *Biochem Pharmacol.* **71,** 713–721, doi: 10.1016/j.bcp.2005.12.017 (2006).
36. Fan, Y. *et al.* Evolution of hepatic steatosis to fibrosis and adenoma formation in liver-specific growth hormone receptor knockout mice. *Frontiers in endocrinology* **5,** 218, doi: 10.3389/fendo.2014.00218 (2014).
37. Koonen, D. P. *et al.* Increased hepatic CD36 expression contributes to dyslipidemia associated with diet-induced obesity. *Diabetes* **56,** 2863–2871, doi: 10.2337/db07-0907 (2007).
38. Zhou, J. *et al.* Hepatic fatty acid transporter Cd36 is a common target of LXR, PXR, and PPARgamma in promoting steatosis. *Gastroenterology* **134,** 556–567, doi: 10.1053/j.gastro.2007.11.037 (2008).

39. Moran-Salvador, E. *et al.* Role for PPARgamma in obesity-induced hepatic steatosis as determined by hepatocyte- and macrophage-specific conditional knockouts. *FASEB journal: official publication of the Federation of American Societies for Experimental Biology* **25,** 2538–2550, doi: 10.1096/fj.10-173716 (2011).
40. Kotronen, A. *et al.* Hepatic stearoyl-CoA desaturase (SCD)-1 activity and diacylglycerol but not ceramide concentrations are increased in the nonalcoholic human fatty liver. *Diabetes* **58,** 203–208, doi: 10.2337/db08-1074 (2009).
41. Jensen-Urstad, A. P. & Semenkovich, C. F. Fatty acid synthase and liver triglyceride metabolism: housekeeper or messenger? *Biochimica et biophysica acta* **1821,** 747–753, doi: 10.1016/j.bbalip.2011.09.017 (2012).
42. Trauner, M., Arrese, M. & Wagner, M. Fatty liver and lipotoxicity. *Biochimica et biophysica acta* **1801,** 299–310, doi: 10.1016/j.bbalip.2009.10.007 (2010).
43. Yeh, Y. T., Lee, K. T., Tsai, C. J., Chen, Y. J. & Wang, S. N. Prolactin promotes hepatocellular carcinoma through Janus kinase 2. *World J Surg.* **36,** 1128–1135, doi: 10.1007/s00268-012-1505-4 (2012).
44. Stiedl, P. *et al.* Growth hormone resistance exacerbates cholestasis-induced murine liver fibrosis. *Hepatology* **61,** 613–626, doi: 10.1002/hep.27408 (2015).
45. Guevara-Aguirre, J. & Rosenbloom, A. L. Obesity, diabetes and cancer: insight into the relationship from a cohort with growth hormone receptor deficiency. *Diabetologia* **58,** 37–42, doi: 10.1007/s00125-014-3397-3 (2015).
46. Buchert, M., Burns, C. J. & Ernst, M. Targeting JAK kinase in solid tumors: emerging opportunities and challenges. *Oncogene*, doi: 10.1038/onc.2015.150 (2015).
47. Sanyal, A. J. *et al.* A pilot study of vitamin E versus vitamin E and pioglitazone for the treatment of nonalcoholic steatohepatitis. *Clin Gastroenterol Hepatol.* **2,** 1107–1115 (2004).
48. Veal, E. A., Toone, W. M., Jones, N. & Morgan, B. A. Distinct roles for glutathione S-transferases in the oxidative stress response in Schizosaccharomyces pombe. *The Journal of biological chemistry* **277,** 35523–35531, doi: 10.1074/jbc.M111548200 (2002).
49. Bourgeais, J. *et al.* Oncogenic STAT5 signaling promotes oxidative stress in chronic myeloid leukemia cells by repressing antioxidant defenses. *Oncotarget* (2016).
50. Naik, A., Kosir, R. & Rozman, D. Genomic aspects of NAFLD pathogenesis. *Genomics* **102,** 84–95, doi: 10.1016/j.ygeno.2013.03.007 (2013).
51. Dai, G. *et al.* Retinoid X receptor alpha Regulates the expression of glutathione s-transferase genes and modulates acetaminophen-glutathione conjugation in mouse liver. *Molecular pharmacology* **68,** 1590–1596, doi: 10.1124/mol.105.013680 (2005).
52. Dawson, M. A. *et al.* JAK2 phosphorylates histone H3Y41 and excludes HP1alpha from chromatin. *Nature* **461,** 819–822, doi: 10.1038/nature08448 (2009).
53. Nilsson, J., Bjursell, G. & Kannius-Janson, M. Nuclear Jak2 and transcription factor NF1-C2: a novel mechanism of prolactin signaling in mammary epithelial cells. *Mol Cell Biol.* **26,** 5663–5674, doi: 10.1128/MCB.02095-05 (2006).
54. Lobie, P. E. *et al.* Constitutive nuclear localization of Janus kinases 1 and 2. *Endocrinology* **137,** 4037–4045, doi: 10.1210/endo.137.9.8756581 (1996).
55. Engblom, D. *et al.* Direct glucocorticoid receptor-Stat5 interaction in hepatocytes controls body size and maturation-related gene expression. *Genes Dev* **21,** 1157–1162, doi: 10.1101/gad.426007 (2007).


## Acknowledgements

We thank Safia Zahma and Margit Gogg-Kamerer for their excellent technical assistance. This work was supported by grant SFB F28 (F2807-B20) and SFB F47 (F4707-B20) from the Austrian Science Fund (FWF).

## Author Contributions

M.T. designed and performed experiments, analysed and interpreted data, acquired data and wrote the manuscript. K.M.M. performed experiments, analyses and interpretation of data, and contributed to the writing of the manuscript. S.M.K. performed hepatic fatty acid analysis; N.G.-S. analysed tumour sections; T.M. performed microarray analysis; D.K. performed Western blot and siRNA experiments; J.B. performed part of qRT-PCR experiments; J.P.-P. contributed to ROS measurement in liver tissue; K.F. contributed to initiation of this project and performed first analysis of the mice; D.S. isolated immortalized $p19^{ARF-/-}$ hepatocytes and M.S. executed immunohistochemical stainings. L.M.T., M.H.H. and J.H. were responsible for professional analysis of histologic sections and critically revised the manuscript. E.Z.-B. provided financial support and recorded data with M.T., and critically revised the manuscript. K.-U.W., W.M., F.G., X.H., L.K. and A.V.K. critically revised the manuscript for important intellectual content. R.M. was responsible for study concept and supervision, analyses and interpretation of data, critically revised the manuscript, and acquired funding. All authors had final approval of the submitted version.

## Additional Information

**Supplementary information** accompanies this paper at http://www.nature.com/srep

**Competing financial interests:** The authors declare no competing financial interests.

**How to cite this article**: Themanns, M. *et al.* Hepatic Deletion of Janus Kinase 2 Counteracts Oxidative Stress in Mice. *Sci. Rep.* **6**, 34719; doi: 10.1038/srep34719 (2016).

This work is licensed under a Creative Commons Attribution 4.0 International License. The images or other third party material in this article are included in the article's Creative Commons license, unless indicated otherwise in the credit line; if the material is not included under the Creative Commons license, users will need to obtain permission from the license holder to reproduce the material. To view a copy of this license, visit http://creativecommons.org/licenses/by/4.0/

© The Author(s) 2016